A rapid two-photon fabrication of tube array using an annular Fresnel lens

Chenchu Zhang,[1] Yanlei Hu,[1,2,*] Jiawen Li,[1,2,3] Guoqiang Li,[1] Jiaru Chu,[1] and Wenhao Huang[1]

[1]*Department of Precision Machinery and Precision Instrumentation, University of Science and Technology of China, Hefei 230026, China*

[2]*These authors contributed equally to the paper.*

[3]*jwl@ustc.edu.cn*

[*]*huyl@ustc.edu.cn*

Abstract: A rapid method of fabricating microscopic tubular structures via two-photon polymerization is presented. Novel Fresnel lens is designed and applied to modulate the light field into a uniform ring pattern with controllable diameters. Comparing with the conventional holographic processing method, Fresnel lens shows higher uniformity and better flexibility, while easier to generate. This versatile method provides a powerful solution to produce tube structure array within several seconds.

OCIS codes: (180.4315) Nonlinear microscopy; (190.4180) Multiphoton processes; (220.4000) Microstructure fabrication; (220.4610) Optical fabrication.

References and links

1. E. J. Smith, S. Schulze, S. Kiravittaya, Y. Mei, S. Sanchez, and O. G. Schmidt, "Lab-in-a-Tube: Detection of Individual Mouse Cells for Analysis in Flexible Split-Wall Microtube Resonator Sensors," Nano Lett. **11**(10), 4037–4042 (2011).
2. G. Huang, Y. Mei, D. J. Thurmer, E. Coric, and O. G. Schmidt, "Rolled-up transparent microtubes as two-dimensionally confined culture scaffolds of individual yeast cells," Lab Chip **9**(2), 263–268 (2009).
3. K. Takei, T. Kawashima, T. Kawano, H. Kaneko, K. Sawada, and M. Ishida, "Out-of-plane microtube arrays for drug delivery--liquid flow properties and an application to the nerve block test," Biomed. Microdevices **11**(3), 539–545 (2009).
4. X. Yang, L. Wang, and S. Yang, "Facile route to fabricate large-scale silver microtubes," Mater. Lett. **61**(14-15), 2904–2907 (2007).
5. D. J. Thurmer, C. Deneke, Y. Mei, and O. G. Schmidt, "Process integration of microtubes for fluidic applications," Appl. Phys. Lett. **89**(22), 223507 (2006).
6. S. Kawata and H. Sun, "Two-photon photopolymerization as a tool for making micro-devices," Appl. Surf. Sci. **208**, 153–158 (2003).
7. K. Lee, R. H. Kim, D. Yang, and S. H. Park, "Advances in 3D nano/microfabrication using two-photon initiated polymerization," Prog. Polym. Sci. **33**(6), 631–681 (2008).
8. S. Matsuo, S. Juodkazis, and H. Misawa, "Femtosecond laser microfabrication of periodic structures using a microlens array," Appl. Phys., A Mater. Sci. Process. **80**(4), 683–685 (2005).
9. T. Kondo, S. Matsuo, S. Juodkazis, and H. Misawa, "Femtosecond laser interference technique with diffractive beam splitter for fabrication of three-dimensional photonic crystals," Appl. Phys. Lett. **79**(6), 725–727 (2001).
10. H. Takahashi, S. Hasegawa, A. Takita, and Y. Hayasaki, "Sparse-exposure technique in holographic two-photon polymerization," Opt. Express **16**(21), 16592–16599 (2008).
11. Y. Hayasaki, T. Sugimoto, A. Takita, and N. Nishida, "Variable holographic femtosecond laser processing by use of a spatial light modulator," Appl. Phys. Lett. **87**(3), 031101 (2005).
12. S. Hasegawa, Y. Hayasaki, and N. Nishida, "Holographic femtosecond laser processing with multiplexed phase Fresnel lenses," Opt. Lett. **31**(11), 1705–1707 (2006).
13. J. Amako, H. Miura, and T. Sonehara, "Speckle-noise reduction on kinoform reconstruction using a phase-only spatial light modulator," Appl. Opt. **34**(17), 3165–3171 (1995).
14. N. J. Jenness, R. T. Hill, A. Hucknall, A. Chilkoti, and R. L. Clark, "A versatile diffractive maskless lithography for single-shot and serial microfabrication," Opt. Express **18**(11), 11754–11762 (2010).
15. C. Hnatovsky, V. G. Shvedov, W. Krolikowski, and A. V. Rode, "Materials processing with a tightly focused femtosecond laser vortex pulse," Opt. Lett. **35**(20), 3417–3419 (2010).
16. E. Stankevicius, T. Gertus, M. Rutkauskas, M. Gedvilas, G. Raciukaitis, R. Gadonas, V. Smilgevicius, and M. Malinauskas, "Fabrication of micro-tube arrays in photopolymer SZ2080 by using three different methods of a

#204806 - $15.00 USD Received 15 Jan 2014; revised 30 Jan 2014; accepted 30 Jan 2014; published 12 Feb 2014

direct laser polymerization technique," J. Micromech. Microeng. **22**(6), 065022 (2012).
17. S. Kawata, H. B. Sun, T. Tanaka, and K. Takada, "Finer features for functional microdevices," Nature **412**(6848), 697–698 (2001).
18. S. D. Gittard, A. Nguyen, K. Obata, A. Koroleva, R. J. Narayan, and B. N. Chichkov, "Fabrication of microscale medical devices by two-photon polymerization with multiple foci via a spatial light modulator," Biomed. Opt. Express **2**(11), 3167–3178 (2011).

1. Introduction

Due to novel functions in the development of advanced devices and systems, microscopic tubular structures have attracted significant interest in many important practical fields such as biologic sensing [1], cell controlling [2], localized drug delivery [3], catalysts [4], and other microfluidic applications [5].

Two-photon polymerization (TPP) has been proved to be an effective method for fabricating microscopic tubular structure [6]. In TPP, tightly cofined instant photo polymerization process via nonlinear absorption of light is initiated in a photosensitive material by closely focused pulsed laser. Material modification only occurs in the vicinity of laser beam waist. So that the size of voxel can be close to the diffraction limit. And real 3D microstructures with high resolution can be made by using a layer by layer accumulating technique [7]. However, the main drawback of TPP technique is its low fabrication efficiency caused by the raster scanning strategy, which seriously restricts its applications. To overcome this problem, researchers convert the single beam into beam array by microlens arrays (MLAs) [8] or diffractive beamsplitters [9], or introducing spatial light modulator (SLM) like liquid crystal on silicon (LCoS) to produce adjustable multi-foci by loading computer generate hologram (CGH) [10,11] or multiplexed phase Fresnel lens [12]. The number and distribution of foci array can be easily controlled by changing the phase pattern loaded on SLM. But for these methods, as all foci follow the same scanning path, only array with the same structures can be achieved. So a single-exposure mode is desired to enhance the flexibility and efficiency of TPP. As the LCoS modifies the phase of incident light, a continuous light field in focal plane has serious speckle noise [13], which ultimately results in flawed and disjointed structures. A time-averaged corrective technique using tens of CGHs successively loaded on LCoS has been used to eliminate the speckle noise and fabricate structures with high quality [14]. With this technique, Jenness et al. presented an approach to fabricate patterns using the single-shot mode with the exposure time of 10 seconds. At the same time, researchers have applied annular beam like optical vortex to fabricate microscopic tubular structure [15]. Stankevicius et al. presented and compared several approaches for producing microtube structures using TPP technology [16], including direct laser writing (DLW), optical vortices (OV) and holographic lithography (HL). But none of these can combine flexibility, fabrication efficiency and structure quality together.

In this paper, a novel annular Fresnel lens is designed and applied to modulate the light field into a uniform ring pattern with continuous controllable diameters. Furthermore, we also propose an efficient approach for producing tube structure array within several seconds.

2. Theory

As we all know, the phase transformation of spherical Fresnel lens is the same with that of spherical lens, which is $t = exp[-ik(r^2) / 2z]$. Here, r is the distance to the center of lens. z is the distance from lens back surface to the observation plane. And k is the wave number. Thus, spherical Fresnel lens (FL) can also focus light into a single point similar to the focusing ability of simple spherical lens. What's more interesting, the focus field of an annular Fresnel lens (AFL) is ring-shaped, which could be used to directly print annular patterns.

#204806 - $15.00 USD Received 15 Jan 2014; revised 30 Jan 2014; accepted 30 Jan 2014; published 12 Feb 2014

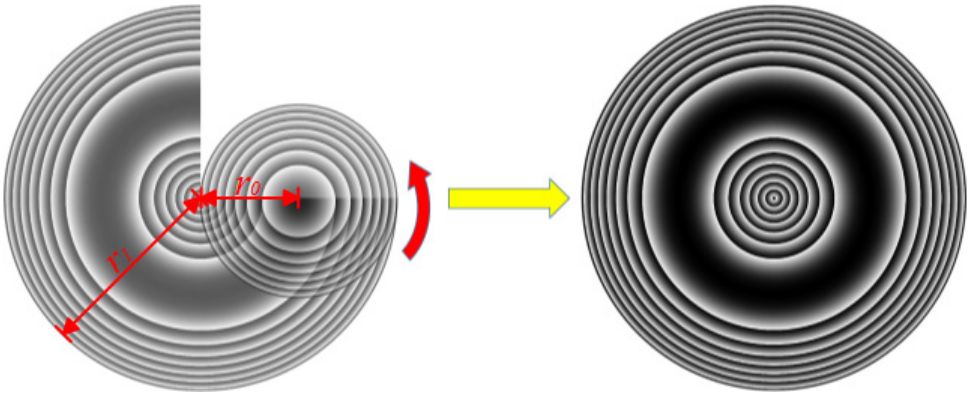

Fig. 1. The left is the diagrammatic sketch of generation process of AFL. The smaller circle is FL. r_0 is the shift distance of FL, which is the same to the radius of FL here. r_1 is the radius of AFL. Red arrow shows the moving direction of FL. And the right is the obtained AFL.

AFL can be described as a conventional FL shifting from the center with a distance r_0, then rotating around the center. As is shown in Fig. 1, r_1 is the radius of the AFL and r_0 is chosen to be half of r_1 here. If r_1 is larger than it is necessary, some parts of FL will overlap or out of the boundary of AFL during the rotating, and these parts will be cut. Then, the phase of AFL will be $t = exp\left[-ik\left(r - r_0\right)^2 / 2z\right]$.

As described above, the shifting and wiping operation will change the equivalent phase of lens, leading to focus changes from a spot to the ring-shape. Besides, the shift will result in the area of inner zones is smaller than that of outer zones and the 3D shape of focus may become cone-like because of the unbalance in the area of zones.

To further investigate the properties of AFL, we perform a numerical analysis to study its focusing ability with the help of the Huygens-Fresnel diffractive integral. The propagation field at the observation plane can be deduced from the initial field at the backside of AFL, according to the following expression:

$$E\left(x,y,z\right) = \frac{exp\left(ikz\right)}{i\lambda z}\int\int_{-\infty}^{\infty} E\left(x_1,y_1\right) exp\left\{\frac{ik}{2z}\left[\left(x - x_1\right)^2 + \left(y - y_1\right)^2\right]\right\} dx_1 dy_1 \qquad (1)$$

Here, x, y are the coordinates for initial field at the backside of the lens, while x_1, y_1 are the coordinates at the observation plane. z is the distance from lens back surface to the observation plane. And k is the wave number. To better simulate the AFL displaying on SLM, we pixelate the AFL with the pixel size of 8μm × 8μm, which is the same with the SLM used in the experiment.

#204806 - $15.00 USD Received 15 Jan 2014; revised 30 Jan 2014; accepted 30 Jan 2014; published 12 Feb 2014

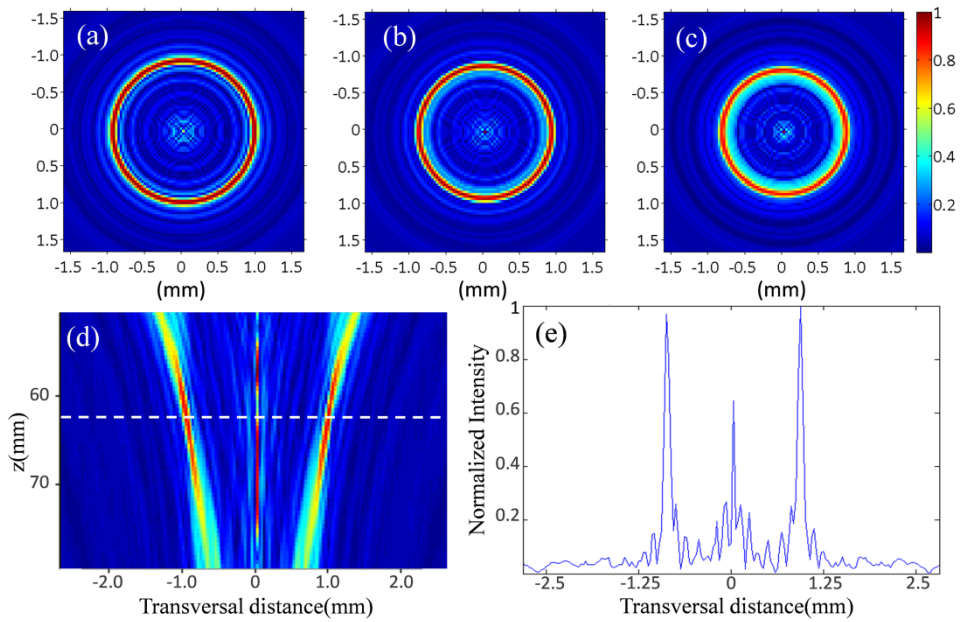

Fig. 2. Simulation results of illuminated field in sagittal plane at (a) $z = 0.95f$, (b) $z = f$, (c) $z = 1.05f$ and (d) meridian plane containing the optical axis; (e) intensity distribution at focal plane.

Figure 2 is the simulation result of an AFL with its 0 order width is 250 pixels and the radius of 0 order zone is 210 pixels. It has 2 inner zones and 5 outer zones. And the focal length is 630mm. According to the simulation, it can be seen that the light field distribution in the observation plane is a ring (Figs. 2(a)–(c)). Although the illumination fields go through scattering near the observation plane, it still retains the ring-shape and continuity, which is very different from CGH. This property makes it possible to fabricate an uninterrupted 3D structure using AFL by single-exposure approach. We also calculate the uniformities of 3 focal rings, which are 90.02% at $z = 0.95f$, 87.52% at $z = f$ and 91.21% at $z = 1.05f$. The uniformity can meet the requirement for fabrication, which is demonstrated in the following experiment. The radius of ring shown in Fig. 2(b) is 0.88mm with the Full Width at Half Maximum (FWHM) of ring line is 24μm. Figure 2(d) is the irradiance for a meridian plane containing the optical axis. It shows that the radius of ring decreased along the light propagation direction and there is an undesired irradiance in the center of ring. White dots show the intensity peak of annular light field which is defined to be the focal plane of AFL. Figure 2(e) shows the light intensity of focal plane, in which the intensity of ring is 1.5 times higher than that of the center beam. The center beam would influence the polymerization of photoresist in some case, so a high-pass filter is used in our experiment to prevent center beam from passing through. The simulation result shows AFL can generate annular light field with a sharp intensity peak, which can enhance the energy density of focus and be very useful in fabricating high resolution microscopic structures.

Table 1. Simulation results of 5 AFLs with different 0 order zone width

0 order width(pixels)	100	150	200	250	300
Number of zones of AFL	30	12	7	5	3
Depth of focus(mm)	10	45	140	340	730
Focal length(mm)	95	230	405	630	885

We choose 5 AFLs with different focal lengths, as is shown in Table 1. These AFLs are created by FLs with the same radius r_1 and shifting distance r_0, the only difference between these FLs is the width of 0 order zone changing from 100 to 300 pixels. Three properties are

#204806 - $15.00 USD Received 15 Jan 2014; revised 30 Jan 2014; accepted 30 Jan 2014; published 12 Feb 2014

measured here: Number of zones of AFL is the number of zones out of the 0 order zone. Depth of focus is the distance between two planes in which the maximum intensity of ring focus is half of that at focal plane. Focal length is the distance between AFL and focal plane. Because of the total area available of SLM is 1080 × 1080 pixels, the number of zones will decreases when the 0 order width increases. And this would result in a great increase of depth of focus. It means that the focus generated by AFL with more zones will produce smaller voxel size in TPP fabrication [17], which is more suitable for producing flexible 3D structures. Beside this, the focal length of AFL is strictly follows the rule: $f_a / f_b = (\rho_a / \rho_b)^2$. Here ρ_a, ρ_b are the width of 0 order zone in FL a and b. In conclusion, the quality of light field in focal plane depends on the number of zones of AFL, and AFL with more zones is more suitable for TPP fabrication. But in experiment, the short focal length will result in some difficulty in building the optics system. Weighting both, we choose AFL with 5 zones in the following experiment.

3. Experimental setup

The experimental setup is shown in Fig. 3. The laser source is a mode-locked Ti:sapphire ultrafast oscillator(Coherent, Chamleon Vision-S) with central wavelength at 800 nm, pulse duration of 75 fs, and repetition rate at 80 MHz. The average power is about 3W, modulated by a power attenuator consisted of a half wave plate and a Glan laserprism. After passing a beam expander, the beam slightly over fills the active area of SLM to ensure modulation effect. The SLM (Holoeye, pluto NIR-2) has 1920 × 1080 pixels, with each pitch of 8μm. Central 1080 × 1080 pixels are used in this work. The Fresnel lens displayed on the SLM has 256 gray levels corresponding to phase modulation from 0 to 2π. A high-pass filter is placed at focal plane of AFL to block the "central light". The remaining of the modulated beam is collected by a collimating lens and focused through a microscope objective (100 × , 0.9 NA) into sample plane. The photoresist used in this work is SZ-2080 (provided by IESL-FORTH, Greece).

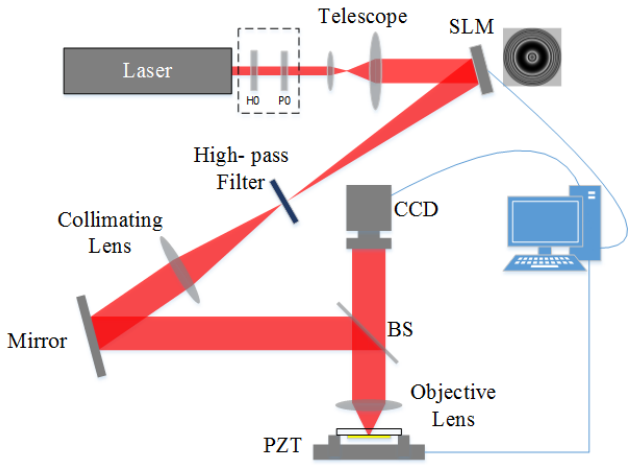

Fig. 3. Diagram of the laser system. H0 is a half wave plate. P0 is a Glan laserprim. AFL is loaded on SLM. A high-pass filter is placed at the focus of AFL to block the center beam.

4. Result and discussion

Figure 4(a) shows a 6 × 6 array of tube structures, each structure is fabricated with a single exposure of 400ms. The distance between adjacent structures is 40μm and the diameter at the top of tube is ~25μm. Figure 4(b) shows the top view of the array. By controlling the irradiated region in x-y plane via translational stages, this array is made within 15 seconds, while it takes tens of seconds to fabricate a single tube by conventional DLW TPP method [16].

#204806 - $15.00 USD Received 15 Jan 2014; revised 30 Jan 2014; accepted 30 Jan 2014; published 12 Feb 2014

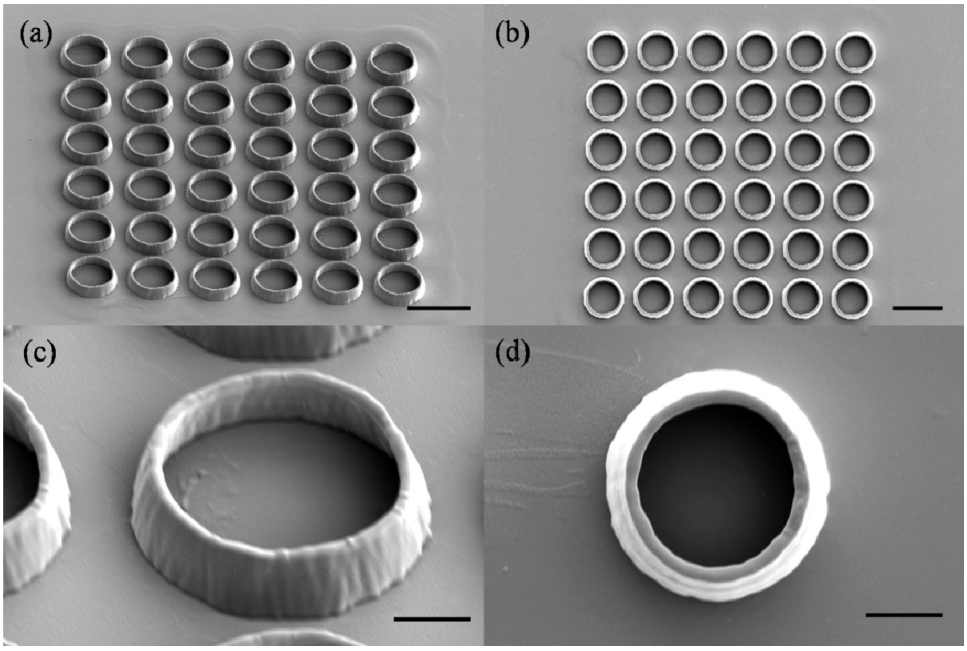

Fig. 4. SEM images of tube array fabricated using the described method with a 100x objective. (a) Arrays captured at 45°; (b) arrays captured at top view; (c) SEM image of an individual structure of array; (d) top view of another individual structure. Scale bars are 40μm in (a), (b) and 10μm in (c), (d).

As shown in Fig. 4(c), the radius of an individual structure decreases with its height rises. It agrees with the simulation result in the meridian plane of AFL. The height of the tube is determined by the parameter in spin coating process. In detail, with 10 seconds slope to 4000 rpm, and keeping this rpm for 45 seconds, the thickness of photoresist is about 8.7μm, which is also the height of tube. The top view of an individual tube is shown in Fig. 4(d). It shows the width of tube at the top is ~1.5μm. And the uniformity of width is 92.6%, which is satisfied in the use of cell feeding [18], drug delivery [3] and so on.

To further study the 3D profile of this structure, we fabricate a tube in the sample prepared with drop casting. The result is achieved using the power of 550 mW and exposure time of 400 ms (see Fig. 5). The tube is a little bit like a taper, as we have discussed above. The thickness of tube wall is related to the intensity distribution of the annular light field, which is ~1.5μm thick in this experiment. Although the intensity uniformity of the ring-shape has been proved to be ~90% in theory, some small deviations (e.g., the peak of gauss beam does not illuminate exactly the center of AFL, and beam axis may have a slight misalignment of the vertical axis of the photoresist surface) will result in the out-of-flatness in the top. The height of polymerized region is~30μm. The long polymerized region along the optical axis is corresponding to the simulation result of focus shape. The large polymerized region is useful when we want to get tube with certain height. But it will become a problem when we want to adopt the layer by layer approach. Fortunately, as we simulated above, shorter focal length can be achieved by choosing an AFL with more zones.

#204806 - $15.00 USD Received 15 Jan 2014; revised 30 Jan 2014; accepted 30 Jan 2014; published 12 Feb 2014

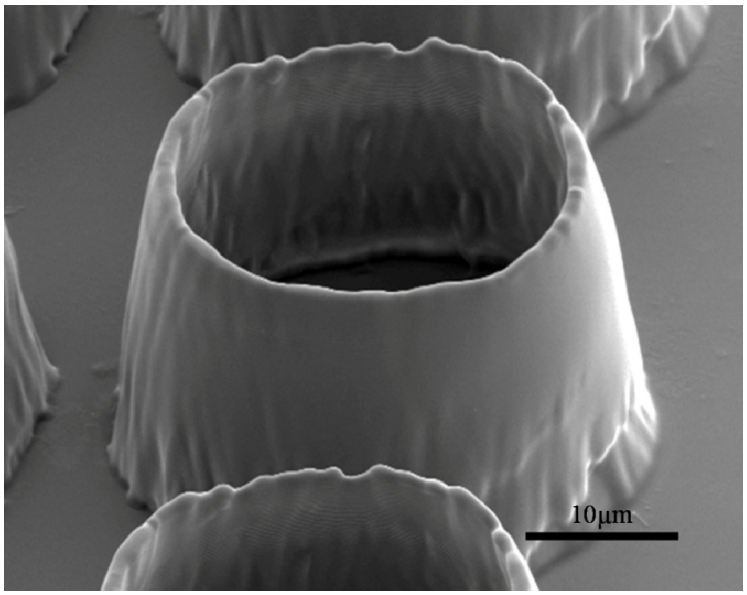

Fig. 5. SEM images of a 3D tube pattern fabricated using AFL.

In conventional multibeam fabrication, all focuses follow the same movement route determined by translational stages. In this way, the individual structures must be identical. By applying AFL, the diameter of structures can be controlled by changing the radius of 0-order zone. Figure 6(a) shows tube array with varies radius. Translational stages and CGH displaying on SLM are synchronously controlled to fabricate contiguous tube structures with arbitrary radius. As this 3 × 6 array is achieved within 9 seconds, arrays with various structures are proved to be made without reduction in efficiency. Figure 6(b) is the top view of this tube array. As we measured, the radii of tubes are 13.4μm, 15.8μm, 18.2μm, 20.6μm, 23.0μm and 25.4μm, corresponding to the radii of 0 order zone varies from 110 pixels to 210 pixels, as shown in Fig. 6(c). The dot lines show the linear relationship of radius between AFL and fabricated structures. So the width of tube can vary in a very large range up to ~65μm in theory as the range of radius of 0-order zone is up to 540 pixels, which means that we can get tube array with radius varies in a very wide range just in seconds.

#204806 - $15.00 USD Received 15 Jan 2014; revised 30 Jan 2014; accepted 30 Jan 2014; published 12 Feb 2014

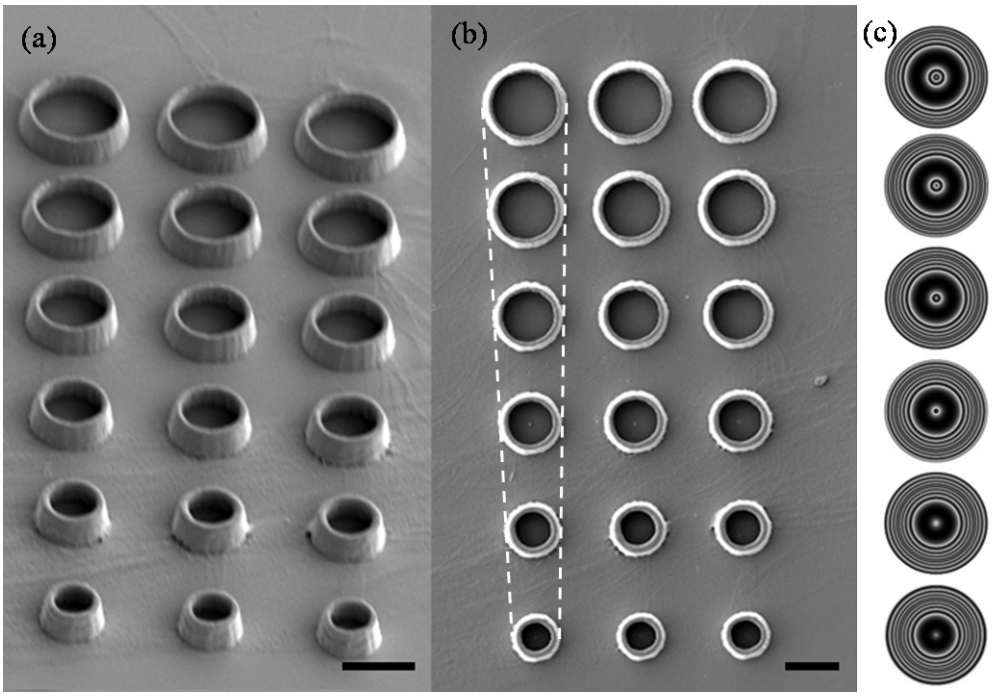

Fig. 6. SEM images of tube array with various radius. (a) Image captured at 45°; (b) image captured at 0°; (c) the AFLs used in fabricating tube with different radius. Scale bars are 20μm.

5. Conclusion

We designed a novel annual Fresnel lens which can generate ring-shape light field in the focal plane. By using this Fresnel lens, a single exposure technique for the fabrication of tube structure array via two-photon polymerization is demonstrated. This technique is much faster and more flexible than the conventional parallel fabrication using array of beam spots. We anticipate this method will be used in fabrication medical micro-devices to be used in the field of cell feeding, biological screening and so on.

Acknowledgments

This work is supported by National Science Foundation of China (No. 51275502), China Postdoctoral Science Foundation funded project (No. 2012M511416 and 2012M521245) and the Fundamental Research Funds for the Central Universities (KB2090090001).

#204806 - $15.00 USD Received 15 Jan 2014; revised 30 Jan 2014; accepted 30 Jan 2014; published 12 Feb 2014